Biophysical Chemistry 13 (1981) 151–165
North-Holland Publishing Company

INTERACTION OF THE RUTHENIUM RED CATION WITH NUCLEIC ACID DOUBLE HELICES

Richard L. KARPEL, Mark S. SHIRLEY and Stephen R. HOLT
Department of Chemistry, University of Maryland Baltimore County,
Catonsville, Maryland 21228, USA

Received 2 September 1980

The hexapositive complex cation ruthenium red very effectively stabilizes DNA and RNA double helices against thermal denaturation. In the presence of nucleic acid helices, this symmetric cation acquires an extrinsic CD spectrum near the wavelength of the dye's maximum absorbance. Competition experiments with single-stranded polyd(T) show this induced CD to be the result of selective binding to helical sites. The preferential affinity of ruthenium red for double helical binding sites is so great that it brings about biphasic absorbance–temperature profiles of polyd(A-T) at low [cation]:[polynucleotide phosphate]. The visible CD signal and fraction of helix melting at the upper transition increases with ruthenium red concentration until approximate charge neutrality is reached. These interactions, which have been studied in detail with the poly(U·U) helix as well as polyd(A-T), are likely largely electrostatic, since sufficient [NaCl] eliminates the biphasic melting of polyd(A-T), renders the ultraviolet absorbance of poly(U) insensitive to ruthenium red, and abolishes the induced CD effects. The biphasic melting of polyd(A-T) at intermediate [dye] is attributed to saturation of remaining double helical segments by cation migration from newly melted regions. Furthermore, virtually no change was observed in the induced CD upon melting through the first transition, whereas the effect is destroyed upon melting through the second transition. A quantitative treatment of the data is used to obtain binding site size and association constant for the complex. The induced effect may prove useful in the exploration of exposed nucleic acid helical structure in such complex particles as nucleosomes or ribosomes.

1. Introduction

Nucleic acids interact with a variety of molecules: enzymes, binding proteins, and many types of small molecules. Among the latter class are cations, such as K^+, Mg^{2+} and spermine (4+). These ions play a role in stabilizing the secondary, tertiary, and quaternary structures of nucleic acids by neutralizing phosphate-phosphate repulsion [1,2]. They are also being increasingly recognized as important mediators of protein-nucleic acid interactions [3,4]. In this respect, the binding of RNA polymerase and of lac repressor to double-stranded DNA were shown to be strongly dependent on $[Na^+]$ and $[Mg^{2+}]$ [4]. The action of helix-destabilizing proteins, which depress T_m by selectively binding to nucleic acid single strands, is also very much affected by cations. The affinity of these proteins for single-stranded DNA and RNA is significantly reduced with increasing $[Na^+]$ [4,5], and cations of higher charge, e.g. Mg^{2+}, are even more effective inhibitors of activity.

Given the importance of small cations in mediating the action of helix-destabilizing and other proteins, the interaction of these ions with nucleic acids and their behavior during heat-induced helix denaturation is of some interest. In particular, cations of high ($\geqslant$2+) charge which have a preferential affinity for helices, can produce extremely broad and even biphasic absorbance-temperature (melting) profiles of homogeneous and heterogeneous double-stranded nucleic acids when present at less than saturating concentrations [6–8]. This behavior has been interpreted as the result of a migration of cations from newly denatured to remaining helical regions [7,8]. Prior to melting, the cations are assumed to be distributed either randomly (non-cooperatively) or evenly (anti-cooperatively, resulting from positive charge repulsions) along the helix lattice. Upon melting, cations bound to helical regions which become denatured migrate to the remaining helix. At some temperature, sufficient melting has occurred so that the remaining helical regions are saturated with cations, and are thus more resistant to heat denaturation than the previous non-saturated states of the helix. The saturated regions eventually melt at higher temperatures, producing a second transition, and thus a biphasic profile.

In order to directly monitor the cation during nucleid acid denaturation, as well as to better understand the binding between cation and helix, we have studied the interaction of ruthenium red, $Ru_3O_2(NH_3)_{14}^{6+}$, with double-stranded DNA (polyd(A-T)) and RNA (poly(U · U)). Along with its extremely high charge, ruthenium red has the advantage of being very highly colored ($\epsilon_{532}^{H_2O} = 6.15 \times 10^4$ ℓ $mole^{-1}$ cm^{-1}, [9]). For a number of years it has been used as a microscopic stain for mucopolysaccharides [10,11]. Ruthenium red appears to be a linear trinuclear ion, with oxygen bridges between the (octahedral) metal centers, $[(NH_3)_5Ru\text{-}O\text{-}Ru(NH_3)_4\text{-}O\text{-}Ru(NH_3)_5]^{6+}$ [12]. An X-ray crystallographic study of an ethylenediamine analog of ruthenium red was shown to have this type of structure [13].

Although ruthenium red itself is not an asymmetric molecule, we show that when bound to helical nucleic acids, an induced visible circular dichroism (CD) spectrum results. This suggests that these non-intercalating dye cations are positioned at asymmetric sites on the helices. Similar induced effects have previously been observed when other dyes were interacted with asymmetric macromolecules [14]. The induced visible CD effect is destroyed upon helix denaturation, and is not seen when the dye is interacted with polynucleotides devoid of secondary structure, e.g. polyd(T). Thus, the induced CD is a probe for the existence of secondary structure, and this result has been exploited for understanding the behavior of the dye cations during heat-induced helix denaturation. Biphasic absorbance-temperature profiles are observed when nucleic acid helices are melted in the presence of sub-saturating levels of ruthenium red. As predicted, the induced CD effect (and thus, cation-helix interaction) is virtually unaffected when the temperature is raised to a point between the two transitions, but is largely destroyed upon melting through the second transition.

2. Materials and methods

2.1. *Ruthenium red*

Commercial ruthenium red chloride samples from Matthey-Bishop or Sigma, on the basis of the magnitude of their absorbance at the dye's maximum (532 nm), were found to be only 10–30% pure. These samples were subjected to the recrystallization procedure of Fletcher et al. [9]. The dye was dissolved in hot (60°C) 0.5 M NH_4OH and centrifuged. The supernatant was cooled, and the resulting crystals were separated by centrifugation, washed sequentially with ice cold H_2O, 95% ethanol, diethyl ether, dried, and then subjected to at least two more rounds of recrystallization. The final product had an absorbance spectrum (determined on a Cary 219 spectrophotometer) identical to that found in the literature, with the apparent aqueous ϵ_{532} determined to be 99% of the published value of 6.15×10^4 ℓ $mole^{-1}$ cm^{-1}, corresponding to $\epsilon_{532}^{Ru} = 2.05 \times 10^4$ ℓ $mole^{-1}$ cm^{-1} [9]. Stock aqueous solutions of this material stored frozen under nitrogen at −20°C showed no signs of degradation, even after a year of storage. Solutions prepared from the purified, dried material which had been stored dessicated at −20°C occasionally showed some precipitate, but the supernatants displayed the characteristic absorbance spectrum and A_{532}/A_{740} (10.8 ± 0.5, [10]), showed only one paper chromatographic spot [10], and, when interacted with nucleic acids, yielded results identical to those obtained with the previously frozen stock solutions.

2.2. *Polynucleotides*

Polyd(A-T) and poly(U) were obtained from PL Biochemicals and used without further purification. Stock solutions were prepared in the standard 10 mM phosphate (K^+), 0.10 mM Na_2EDTA, pH 7.0 buffer. Concentrations were determined using, for polyd(A-T), ϵ_{260} $(= \epsilon_{262}) = 6.65 \times 10^3$ ℓ $mole^{-1}$ cm^{-1} [15], and for poly(U), $\epsilon_{261} = 9.4 \times 10^3$ [16]. These nucleic acids were of a size range where T_m is essentially independent of helix length, and no variation was observed among the several samples utilized. All other chemicals used were of reagent or comparable grade.

2.3. Samples for absorbance–temperature profiles

In preliminary experiments, samples of ruthenium red and polynucleotides were prepared in glass culture tubes from stock solutions. However, adsorption of the dye to glass resulted in a loss of A_{532} over several days; henceforth all ruthenium red solutions were prepared in plastic tubes. Fresh stock solutions of ruthenium red in the standard phosphate/EDTA buffer at a concentration of $1-2 \times 10^{-3}$ M were prepared weekly and frozen when not in use. The concentrations of these solutions were checked (at 100–200 fold aqueous dilution) spectrophotometrically at 532 nm before sample preparation. Test samples were prepared in the standard phosphate/EDTA buffer, with NaCl added, as indicated, in the $[Na^+]$ dependence experiments. These solutions were kept in the dark at 4°C, and all measurements were taken within 24–48 hrs of preparation. Na_2EDTA was present to sequester any heavy metal impurities, which might affect T_m. Polynucleotide-ruthenium red samples differing only in $[Na_2EDTA]$, 0.10 and 0.010 mM, gave superimposable absorbance-temperature profiles, and the magnitudes of induced circular dichroism effects were virtually unchanged ($\lesssim 2\%$) by a 100-fold variation in $[Na_2EDTA]$, 0.010 to 1.0 mM.

2.4. Absorbance-temperature profiles

Teflon-stoppered semi-micro quartz cuvettes containing 400 μl of test solutions were placed in a Gilford 2400-2 recording spectrophotometer designed to raise the temperature from 0–95°C at a constant rate, which was generally 25°C/hr in these experiments. Generally, three polynucleotide-ruthenium red samples were melted simultaneously with a reference cuvette containing the standard buffer. Temperature was continually monitored by means of a calibrated thermistor (Yellow Springs Instruments) inserted through a narrow hole in the stopper of the reference cuvette. Absorbance was measured at the wavelength of maximum hyperchromic change, 260 nm for polyd(A-T) and 261 nm for poly(U). To assure that equilibrium melting profiles were obtained, identical samples were occasionally subjected to two different rates of temperature increase and found to possess the same (±1°C) T_m. In addition, it was observed that if during a (steep) melting transition the temperature was repeatedly held constant and then decreased or increased, the resulting absorbance changes followed the temperature change with less than a 1°C lag. T_m values are defined as the inflection points of the transitions as determined by differentiating the measured absorbance-temperature profiles [8]. The reproducibility of the T_m values was ±1°C, except when profiles were very broad, where it was ±2°C.

2.5. Circular dichroism experiments

Measurements of circular dichroism spectra were taken with a JASCO J-40 spectropolarimeter. The cuvette holder of the instrument was adapted to hold rectangular semi-micro quartz cuvettes containing as little as 400 μl of sample, and was connected to an external circulating water bath. Unless otherwise indicated, the cuvette temperature was 25°C for polyd(A-T) samples and 10°C for poly(U) samples. These values corresponded to the initial temperatures of their respective melting profile experiments. Cuvette temperature was determined via a calibrated thermistor probe (Yellow Springs Instruments). Wavelength and CD scale calibration were periodically checked according to the J-40 manual using, respectively, holmium oxide and neodynium glass, and 0.142% (6.10×10^{-3} M) recrystallized d-10-camphorsulfonic acid as standards.

3. Results

Two synthetic nucleic acids, polyd(A-T) and poly(U · U), were chosen for extensive study with the ruthenium red cation. The induced CD effects described below were also observed with a wide variety of synthetic and natural nucleic acid helices, including calf thymus DNA, yeast transfer RNA, and poly(A). We have concentrated on the two synthetic double helices because they exhibit especially low T_m's. Given the heat sensitivity of ruthenium red (see below), polyd-(A-T) and poly(U · U), which denature at relatively low temperatures, are especially well suited for study. Furthermore, these helices were used in a study of the effect of tripositive metal complexes, such as $Co(NH_3)_6^{3+}$ on nucleic acid melting characteristics, and showed biphasic melting behavior at sub-saturating cation concentrations [8]. Ruthenium red, which is a multi-centered metal ammine complex, would be expected to show analogous properties

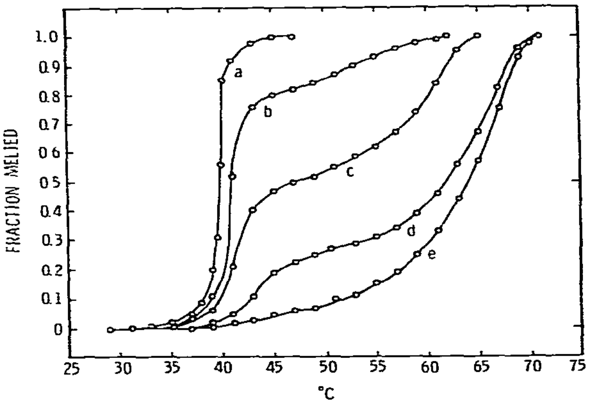

Fig. 1. Effect of ruthenium red on thermal denaturation of polyd(A-T) (7.1 × 10^{-5} M(p)). 0.010 M phosphate (K^+), 0.10 mM Na_2EDTA, pH 7.0. [Dye] : [polyd(A-T)]$_p$ (≡*R*): (a) 0; (b) 0.022; (c) 0.067; (d) 0.101; (e) 0.134.

3.1. Polyd(A-T)

In the absence of ruthenium red, polyd(A-T) displays a monophasic melting profile with a T_m of 41 ± 1°C in the low ionic strength buffer employed. When ruthenium red is added to polyd(A-T) (7.1 × 10^{-5} M(p)), a second, higher melting transition appears in the absorbance temperature profile (fig. 1). At the lowest [cation] : [polynucleotide]$_p$ ratios (≡*R*), only a small amount of helix melts at this higher temperature. As more ruthenium red is added, there is an increase in the amount of helix melting in this upper transition and the melting profile becomes markedly biphasic, until at $R = 0.13$ the profile again becomes monophasic with all the helix melting in the upper transition, with a T_m of 67°C (fig. 1e). Although above an *R* value of 0.13 all of the polyd(A-T) melts at the higher T_m, the transition breadth is greater than that of polyd(A-T) in the absence of the dye. The fraction of helix melting at the higher transition is seen to linearly increase with increasing *R* up to 0.134, suggesting that ruthenium red binds sufficiently tightly to double helices so that, below saturation, any increase in [dye] is an increase in [bound dye] (fig. 2). Likewise, the fraction of helix melting at the lower transition is shown in fig. 2 to decrease linearly with increasing *R*. These results are consistent with the assumed model for cation interaction, which predicts biphasic melting between $R = 0$ and the *R* value corresponding to saturation of the helix by the cations [8]. The linear increase (and decrease) in the fraction melting at the higher (and lower) T_m would thus reflect the increase in the proportion of helix protected against thermal denaturation by the dye molecules.

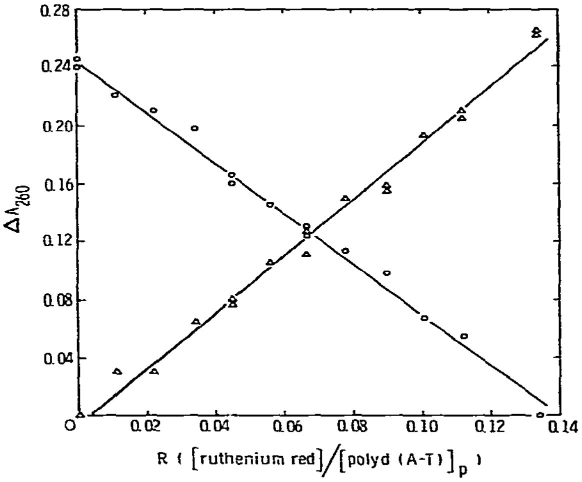

Fig. 2. Variation of hyperchromicity of lower (—○—) and upper (—△—) biphasic melting transitions of polyd (A-T) with increasing *R*. Otherwise, conditions as in fig. 1.

The T_m values for ruthenium red-polyd(A-T) mixtures are plotted versus log [ruthenium red] in fig. 3. The apparent linear dependence of T_m on log [cation] was also observed with the tripositive complexes [8]. The higher transition shows a strong dependence on log [ruthenium red] (dT_m/d log [cation] = 21°C), but the lower transition shows virtually no effect of [ruthenium red] (dT_m/d log [cation] = 4°C). Since the lower T_m reflects helix which is presumably unprotected by the dye cations, these results are consistent with the model presented above.

A very striking property of ruthenium red is the large induced circular dichroism spectrum observed when this symmetric molecule is interacted with the asymmetric nucleic acid helices. Non-interacted ruthenium red and polyd(A-T) possess no visible CD spectrum, but when mixed together a significant induced Cotton effect is seen, with a large positive peak at 562 nm and a relatively small negative peak at 523 nm

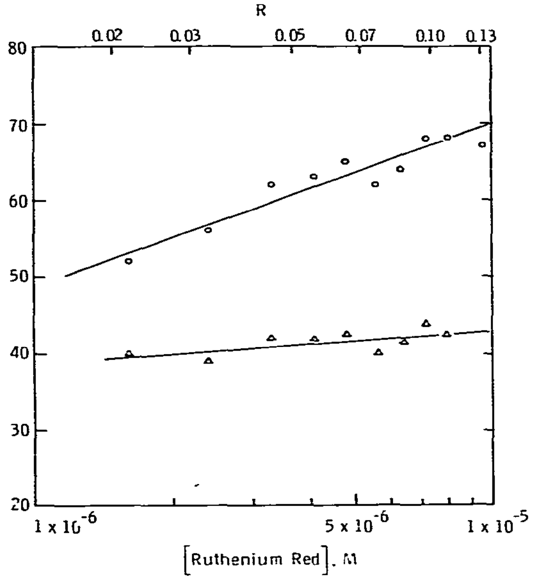

Fig. 3. Variation of polyd(A-T) T_m with increasing [ruthenium red]. Lower transition: –△–; upper transition: –○–. Otherwise, conditions as in fig. 1.

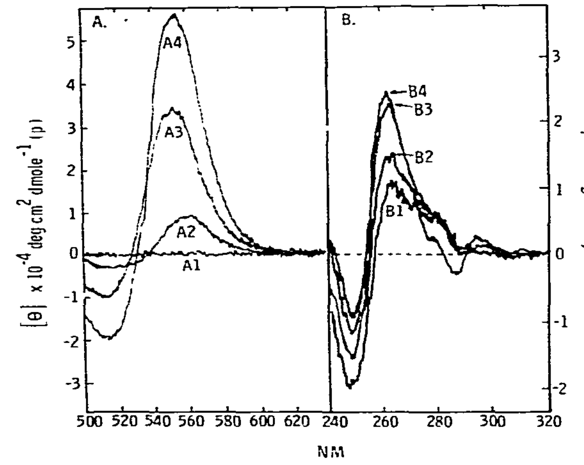

Fig. 4. Circular dichroism spectra of ruthenium red–polyd-(A-T) mixtures at 25°C. R = 0 : A1, B1: R = 0.034 : A2, B2: R = 0.090 : A3, B3: R = 0.134 : A4, B4. Otherwise, conditions as in fig. 1.

(fig. 4). As R increases, there is a monotonic increase in $[\Theta]_{562}$ (calculated with respect to $[\text{polyd(A-T)}]_p$) and a monotonic decrease in $[\Theta]_{523}$ up to a [dye] : $[\text{polyd(A-T)}]_p$ of 0.17, roughly corresponding to the charge neutralization ratio (fig. 5). At higher ruthenium red concentrations ($R > 0.17$), the ellipticity at 562 nm decreases somewhat. This is probably the result of precipitation, which began to be apparent when R exceeded 0.17. Such precipitation may be indicative of DNA condensation to a compact toroidal conformation, which has been observed to occur near the charge neutralization point in the presence of polyamines or $Co(NH_3)_6^{3+}$ [17].

A different plot results if the molar ellipticity at 562 nm is calculated with respect to $[\text{ruthenium red}]_{\text{total}}$ instead of the concentration of nucleotide residues. As seen in the inset of fig. 5, the $[\Theta]_{562}$ with respect to [dye] initially increases rapidly with increasing [dye] up to $R = 0.04$, at which point the slope decreases, and the plot is linear at $0.04 < R < 0.17$. The affinity of ruthenium red for polyd(A-T) is sufficiently high (see below) so that $[\Theta]_{562}$ with respect to [dye] (at $R \leqslant 0.17$), when corrected for the variation in molar ellipticity with respect to [dye], is probably reflective of the density of cation binding to the polynucleotide lattice (see Discussion).

In contrast to the large changes seen in the visible CD, the UV portion of the CD spectrum of polyd(A-T) is affected to a smaller extent by the binding of ruthenium red (figs. 4 and 5). Polyd(A-T) alone at 25°C shows a Cotton effect with a relatively broad positive peak at 262 nm ($[\Theta] = 1.0 \times 10^4$ deg cm^2 dmole^{-1}) and a negative peak at 247 nm. As ruthenium red is added this broad positive peak is sharpened and the magnitude increased up to a maximum value of 2.4×10^4. In addition, at $R = 0.056$ a small shoulder appears on the positive peak at 294 nm and increases as more ruthenium red is added. The negative peak of polyd(A-T) remains unaltered in shape but the absolute value of its molar ellipticity decreases from 1.9×10^4 for polyd(A-T) alone to 0.61×10^4 at $R = 0.224$.

The effect of the cationic dye on T_m would indicate a strong preference for helices. This was demonstrated directly by competition experiments using polyd(T), a structureless single-stranded DNA lacking base stacking [18]. Ruthenium red when added to 8×10^{-5} M(p) polyd(T) shows no visible CD effect at $R = 0.06$ and 0.1, and has only a small effect on the positive and negative UV CD peaks of this polynucleo-

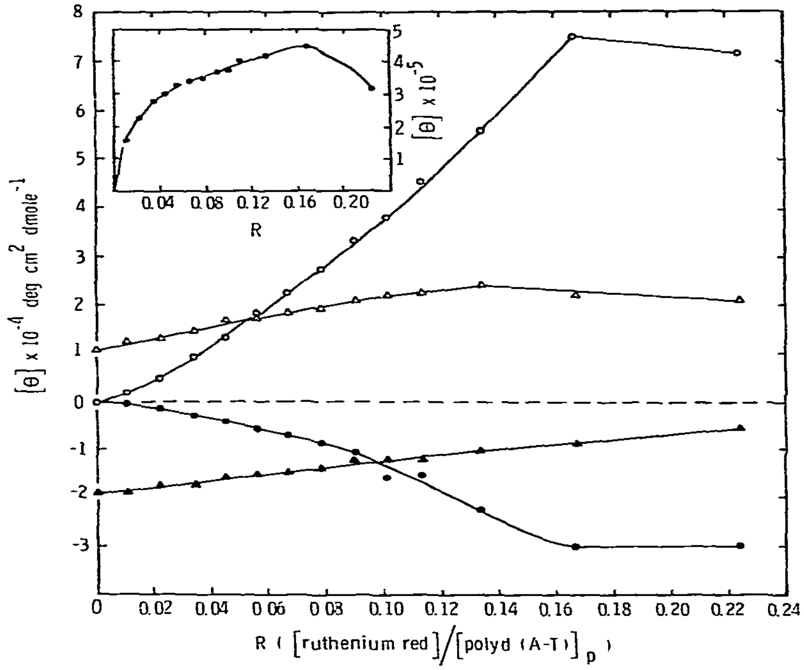

Fig. 5. Variation of ultraviolet and induced visible CD maxima and minima of polyd(A-T) with R at 25°C. With the exception of the inset, ellipticities are calculated with respect to [polyd(A-T)]$_p$. $[\Theta]_{562}$: –○–; $[\Theta]_{262}$: –△–; $[\Theta]_{523}$: –●–; $[\Theta]_{247}$: –▲–. Inset: $[\Theta]_{562}$ is calculated with respect to [ruthenium red]. Otherwise, conditions as in fig. 1.

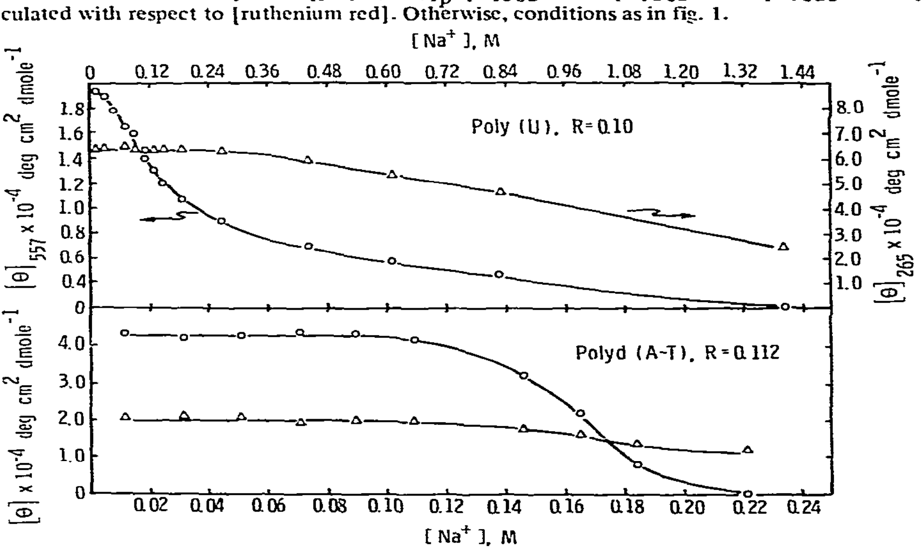

Fig. 6. [Na$^+$] dependence of ultraviolet and induced visible ellipticities of the interaction of ruthenium red with polyd(A-T) (at 25°C) and poly(U) (at 10°C). 8.2×10^{-5} M(p) poly(U), $R = 0.10$; 7.3×10^{-5} M(p) polyd(A-T), $R = 0.112$. Ellipticities are calculated with respect to [nucleic acid]$_p$. Upper panel (poly(U)): $[\Theta]_{557}$: –○–; $[\Theta]_{265}$: –△–. Lower panel (polyd(A-T)): $[\Theta]_{562}$: –○–; $[\Theta]_{262}$: –△–.

tide (<20%, not shown). A 5.6 fold excess of polyd(T) over polyd(A-T) reduced the magnitude of the induced visible CD peak of the polyd(A-T)-ruthenium red complex at $R = 0.067$ by only 12%, and in a 1 : 1 dilution of this mixture, the proportion of polyd(A-T) melting at the lower T_m increased only slightly (50% to 56%). These results indicate that ruthenium red binds much more tightly to double helical structures than to single-stranded nucleic acid coils.

Like the tripositive metal complexes, the interaction of the ruthenium red cation with nucleic acids is strongly dependent on ionic strength. This is observed by the effect of increasing [NaCl] on the induced CD spectra as well as on melting behavior. At $R = 0.112$, where about 60% of maximum induced ellipticity occurs, it is seen that $[\Theta]_{562}$ is invariant up to 0.1 M Na^+ (fig. 6). Between 0.1 and 0.2 M Na^+, $[\Theta]_{562}$ is sigmoidally reduced to 0, with half the induced effect remaining at 0.165 M Na^+. Similar results were obtained at $R = 0.056$. A parallel result was obtained for the effect of salt on T_m. At $R = 0.073$, where the biphasic melting profile is about evenly divided between lower and upper transitions in the absence of added salt, a purely monophasic transition is seen in 0.2 M NaCl (not shown). These results contrast somewhat with those of the trivalent complex-nucleic acid helix study, where 0.1 M Na^+ was sufficient to eliminate the interaction [8].

The behavior of cations during biphasic helix denaturation, as presented in the Introduction, predicts no net change in cation binding during the first transition, but a complete loss of cations bound to nucleic acid across the second transition. The induced CD effect is a direct probe of cation–helix interaction, and thus can be used to test this hypothesis. A polyd(A-T) (7.1×10^{-5} M(p))–ruthenium red solution at $R = 0.067$ was chosen, so that about half the helix would melt at the lower, half at the higher T_m (fig. 2). A CD spectrum was taken at 25°C (well below the onset of melting, fig. 1c), then at 47°C (in between the two transitions), again at 25°C, then at 73°C (where the helix is completely melted), and finally again at 25°C. Spectra were recorded only after the system had attained equilibrium, as judged by constant ellipticity in the ultraviolet. Upon heating to 47°C, the induced CD peak rose by 10%, and the ultraviolet maximum fell by 26%. When cooled to 25°C, the $[\Theta]_{560}$ was within 3% of its original value at that temperature, and $[\Theta]_{262}$ within 4%, indicating reversibility. These results are consistent with the prediction that there is no net change in cation binding, hence no change in the induced effect upon melting through the first transition. The small increase in ellipticity in the visible can be explained in terms of the variation in $[\Theta]$ with respect to [dye] (and hence, with respect to R at constant [nucleic acid], fig. 5, inset). At 47°C, the effective R is really twice the starting value, or 0.134, since half the helix has denatured and, as we have shown above, there is little interaction between dye and single strands. Between $R = 0.067$ and 0.134, $[\Theta]_{562}$ with respect to [ruthenium red] increases by 8% at 25°C, close to the increase observed upon melting through the first transition. Upon heating to 73°C, no visible circular dichroism was observed, and the ultraviolet CD spectrum resembled that of heat-denatured polyd(A-T), with a $[\Theta]_{max}$ at 271 nm and a $[\Theta]_{min}$ at 248 nm [5,19]. Upon cooling again to 25°C, the visible peak was largely unrestored (7%), and the ultraviolet CD spectrum was similar to that obtained for polyd(A-T) in the absence of added ruthenium red (fig. 4).

With total helix denaturation, the induced ellipticity should be destroyed upon melting through the second transition, which is what occurs; however upon cooling, the renaturation of the helix should be accompanied by restoration of the induced effect, which does not occur with polyd(A-T). In this regard, we also observed that the visible absorbance of ruthenium red is irreversibly bleached upon heating above 60°C. This characteristic thermal denaturation of ruthenium red was seen in a number of different buffers, as well as water. The presence of polyd(A-T) had little effect on the rate and extent of bleaching at 60°C. When a polyd-(A-T)–ruthenium red solution ($R = 0.067$) is melted at the standard heating rate of 25°C/hr, the differential visible absorbance-temperature profile ($\Delta A_{532}/\Delta T$ versus T) lags behind the corresponding ultraviolet profile ($\Delta A_{260}/\Delta T$ versus T; fig. 7). The higher T_m in these experiments is thus likely indicative of the helix-stabilizing activity of ruthenium red rather than of the heat sensitivity of the dye. However, since some bleaching (hence decomposition) has occurred prior to the second UV transition (65°C, fig. 7), the higher T_m values are probably not totally reflective of the cation's heat-stabilizing activity. A result analogous to the CD data was obtain-

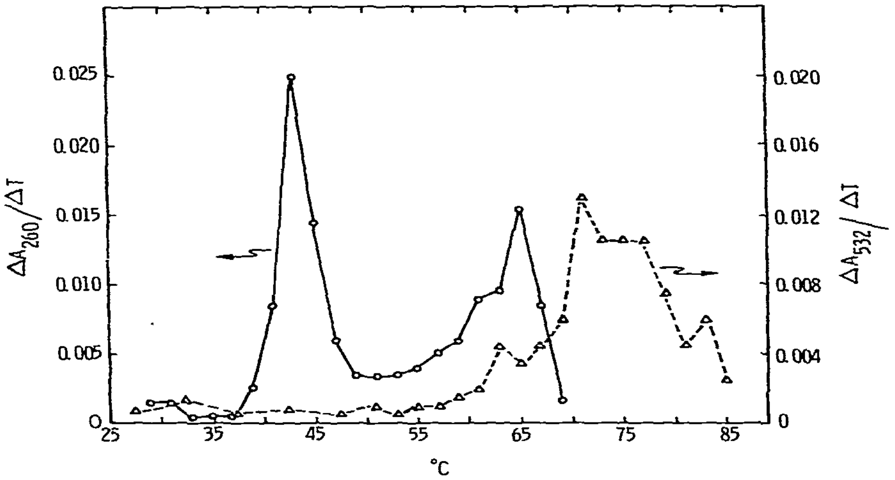

Fig. 7. Differential absorbance-temperature profile of a ruthenium red-polyd(A-T) mixture (R = 0.067). $\Delta A_{260}/\Delta T$: —○—; $\Delta A_{532}/\Delta T$: ——△——. Otherwise, conditions as in fig. 1.

ed when a ruthenium red–polyd(A-T) solution (R = 0.056) was melted through its first transition, then cooled, and remelted through both transitions. The T_m and absorbance change (about half the total hyperchromicity) of the lower transition were reproduced upon remelting, and the higher T_m was equivalent to previous results (fig. 3). However, upon cooling and remelting again, all of the material denatured at the lower T_m (with a hyperchromicity that was 85% of the original, biphasic absorbance change), suggesting that the ruthenium red was destroyed or otherwise altered when the solution was heated through the second transition (>60°C). An unambiguous observation of reversible melting across the upper transition of a biphasic profile was observed in the ruthenium red–poly(U · U) system, where helix denaturation is complete at temperatures below the onset of dye bleaching.

3.2. Poly (U · U)

At low or moderate ionic strengths, poly(U) exists as a random-coiled polymer with no secondary structure [20]. In the presence of low concentrations of spermine (4+) or other highly charged ions, or molar levels of alkali metal ions, this polynucleotide takes on a helical structure at low temperatures [21,22]. It has been shown, via X-ray crystallographic techniques, to be an anti-parallel double helix consistent with a U-U pairing arrangement [23].

In the 0.01 M phosphate–10^{-4} M EDTA buffer used in these studies, poly(U) exhibits no evidence for helical structure, since the ultraviolet absorbance and ellipticity were invariant with temperature. In the presence of ruthenium red, however, the poly(U · U) helix apparently formed since monophasic absorbance temperature profiles were observed. The magnitude of the hyperchromic change increases linearly with [ruthenium red] up to R = 0.08; beyond this point some precipitation occurred and there was a gradual fall-off in the the absorbance change (fig. 8). The actual amount of maximum absorbance change was found to vary slightly from one preparation of poly(U) to another and was 25–35% lower than the maximum hyperchromicity found with spermine (at 2.8×10^{-5} M, R = 0.34). The R value at which the maximum hyperchromic change occurred, 0.08, was the same for all preparations, however, and when normalized against this maximum change the increase in absorbance on melting of all samples was found to depend on [ruthenium red] in the same manner.

Variation of T_m with log [ruthenium red] is approximately linear, with dT_m/d log [dye] = 15°C (fig. 9). Although no biphasic profiles were seen, the ob-

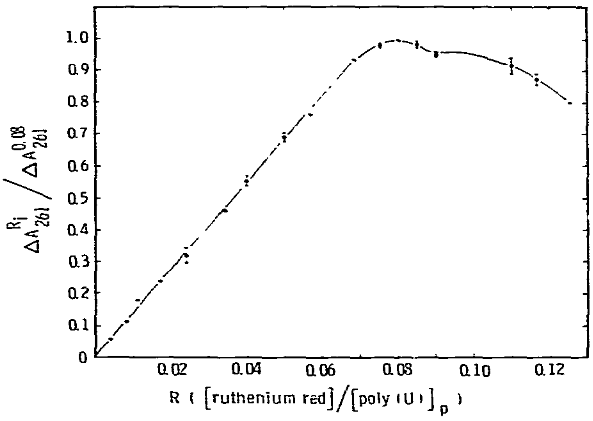

Fig. 8. Dependence of poly(U · U) hyperchromic change as a function of R. The ΔA_{261} values are plotted relative to the maximum ΔA_{261} at $R = 0.08$. $[\text{poly(U)}]_p = 8.2 \times 10^{-5}$ M. Otherwise, coinditions as in fig. 1.

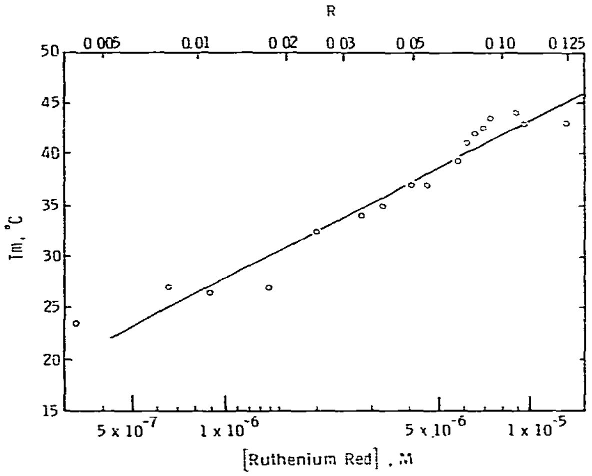

Fig. 9. Variation of poly(U · U) T_m with increasing [ruthenium red]. Otherwise, conditions as in fig. 8.

served absorbance-temperature profiles in reality represent the higher transitions of a melting process where the lower T_m's occur below 0°C. (The T_m for poly(U · U) in 1 M Na^+ is ~5°C, and is <0°C in 0.15 M Na^+ [24]. Since the ionic strength is even lower in these experiments, the T_m in the absence of ruthenium red is likely well below 0°C.) In this light, the hyperchromicity and T_m data parallel the results seen with polyd(A-T).

As with polyd(A-T), interaction of the dye with poly(U) induces a visible circular dichroic effect (fig. 10). The induced effect increases with increasing R, with a concomitant 3-fold increase in $[\theta]_{265}$ at 10°C (fig. 10). The dependence of the visible molar ellipticity

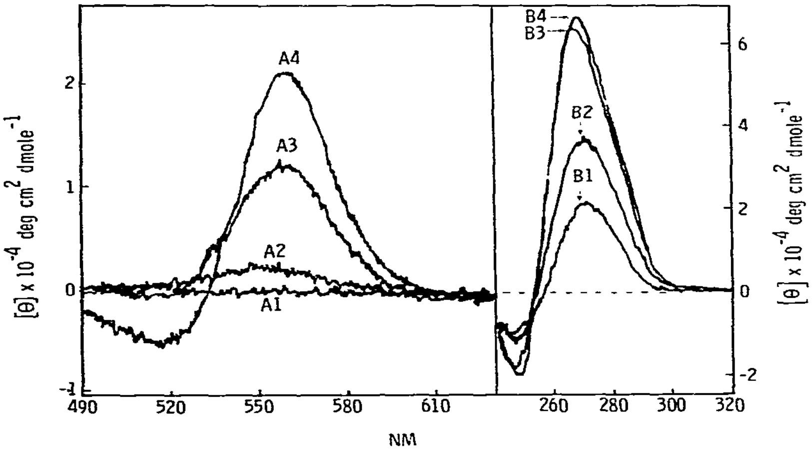

Fig. 10. Circular dichroism spectra of ruthenium red-poly(U) mixtures at 10°C. $R = 0$: A1, B1: $R = 0.024$: A2, B2; $R = 0.080$: A3, B3; $R = 0.110$: A4, B4. Otherwise, conditions as in fig. 8.

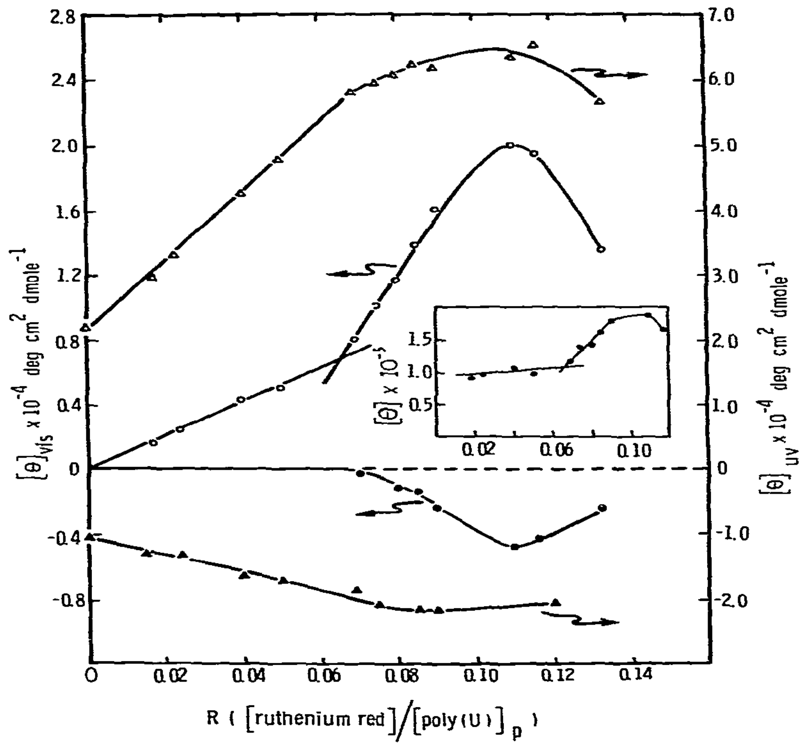

Fig. 11. Variation of ultraviolet and induced visible CD maxima and minima of poly(U) with R at 10°C. With the exception of the inset, ellipticities are calculated with respect to $[\text{poly(U)}]_p$. $[\Theta]_{557}$: —○—; $[\Theta]_{265}$: —△—, $[\Theta]_{515}$: —●—; $[\Theta]_{247}$: —▲—. Inset: $[\Theta]_{557}$ is calculated with respect to [ruthenium red]. Otherwise, conditions as in fig. 8.

(calculated with respect to $[\text{poly(U)}]_p$) on [ruthenium red] however, is different from that observed in the polyd(A-T) system (fig. 11). The ellipticity at 557 nm increases in two linear steps up to a maximum value at $R = 0.11$ with a sharp change of slope at $R = 0.065$. For $R > 0.11$ the magnitude of the induced CD decreases, and precipitation is observed. The molar ellipticity expressed with respect to total added [ruthenium red] shows the change of slope at $R = 0.07$ even more dramatically. The UV circular dichroism spectrum of poly(U) is dramatically affected by the dye, which reflects the formation of the poly(U · U) helix. The positive UV peak increases linearly from a value of 2.2×10^4 deg cm^2 dmole^{-1} at $R = 0$ to 5.8×10^4 at $R = 0.07$, at which point it is about 90% of its maximum value, 6.5×10^4 at $R = 0.11$. In contrast, $[\Theta]_{557}$ (with respect to $[\text{poly(U)}]_p$) at $R = 0.07$ is 35% of its value at $R = 0.11$. It would thus appear that the poly(U · U) helix can nearly fully form at less than saturating levels of dye. This is clearly shown in fig. 12, where, for all R values, the ratio of $[\Theta]_{265}$ (relative to $R = 0$) to $[\Theta]_{265}$ at $R = 0.11$ (relative to $R = 0$) is plotted vs. the ratio of $[\Theta]_{557}$ to $[\Theta]_{557}$ at $R = 0.11$. Two straight lines result, with a point of discontinuity at $R = 0.07$. The large increase in the visible CD at $R > 0.07$, where there is only a small increase in the ultraviolet peak, might reflect a change in the mode of dye binding. Conceivably, the asymmetric environment of the bound ruthenium red at $R < 0.07$ could be different from that at $R > 0.07$, with different modes of binding to the helix (see Discussion).

Unlike polyd(A-T)-dye mixtures, poly(U)–ruthenium red solutions could be melted, cooled, and remelted with virtually no change in accompanying physi-

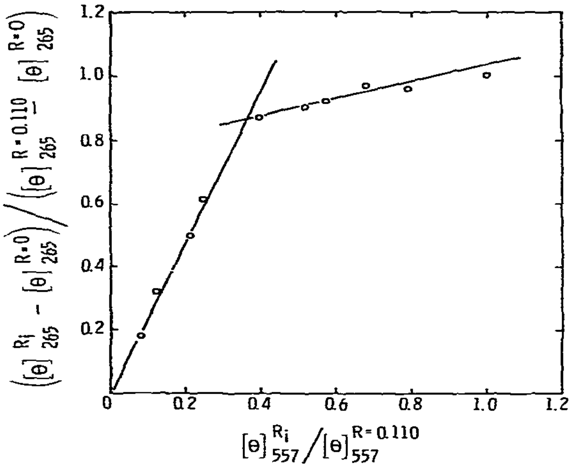

Fig. 12. Dependence of increase in $[\Theta]_{265}$ relative to maximal $[\Theta]_{265}$ (at $R = 0.110$) on increase in $[\Theta]_{557}$ relative to maximal $[\Theta]_{557}$ (at $R = 0.110$) for poly(U) at 10°C. Otherwise, conditions as in fig. 8.

cal properties. Thus, when a mixture at $R = 0.08$ is heated from 10°C to 50°C, (where poly(U · U) is fully denatured), the $[\Theta]_{265}$ is reduced to 24% of its initial value, and the $[\Theta]_{557}$ virtually disappears (~7×10^2 deg cm^2 dmole^{-1}). This is as predicted, since upon melting through the higher transition, the cations no longer remain bound to the nucleic acid. Upon cooling to 10°C, the molar ellipticities at 265 nm and 557 nm are restored to, respectively, 96% and 93% of their original values. Likewise, the hyperchromicity of re-melted solutions was observed to be about 90% of the original ΔA_{261}. Thus, the interaction of ruthenium red with nucleic acid helices is in principle fully reversible, as long as the temperature is not raised to a point where the dye decomposes. The reversible disappearance of the induced CD effect across what is effectively the higher portion of a biphasic transition is consistent with the removal of the cations from the asymmetric helical binding sites.

The [Na$^+$] dependence of ruthenium red-poly(U · U) interaction, as exhibited by changes in induced and ultraviolet ellipticity, is shown in fig. 6 for $R = 0.010$, 10°C. Unlike the polyd(A-T) system, in which helix is always fully formed, a simple sigmoidal dependence on [NaCl] is not seen. The ellipticity at 265 nm is reduced over a broad range of [Na$^+$], reflecting the breakup of the poly(U · U) helix. The dependence of $[\Theta]_{557}$ on [Na$^+$] has an inflection point at 0.12 M Na$^+$, but the effect does not fully disappear until 1.4 M Na$^+$. At this point, the maximum UV ellipticity (2.42×10^4 deg cm^2 dmole^{-1}) is slightly higher than the maximum value for the poly(U) coil (2.20×10^4), suggesting that some small amount of helix remains. (In 1 M Na$^+$, the poly(U · U) helix is not completely (~90%) melted at 10°C [24]). In all probability, the relatively broad dependence of $[\Theta]_{265}$ on [Na$^+$] at >0.24 M Na$^+$ is reflective of the opposing effects of decreasing ruthenium red-poly(U · U) interaction and stabilization of the helix by high [salt]. The relatively abrupt reduction in $[\Theta]_{557}$ (to ~50% of its initial value) but invariant $[\Theta]_{265}$ when [Na$^+$] is raised to 0.24 M indicates that the dye need not be saturating in order to fully stabilize the helix, analogous to the titration results of figs. 10 and 11.

4. Discussion

4.1. Cation site binding and mobility during helix denaturation

Ruthenium red, a symmetric dye cation which displays no circular dichroism when free in solution, shows a very large induced CD effect near its visible absorbance maximum when interacted with DNA or RNA helices. This induced effect must result from an asymmetric environment of the dye chromophore at the helix, and likely reflects direct binding of the dye to (asymmetric) sites on the macromolecule. The binding to helices of certain dyes, such as acridine orange, and the resultant induced effects are strongly influenced by dye self association [14]. The induced effects of other dyes, such as methylene blue, are reflective of macromolecular helical structure [14]. There is no evidence that ruthenium red self-associates, which would be unlikely since it is a highly charged (6+), non-aromatic cation. It seems reasonable, therefore, to view the induced CD effects seen with this dye as a direct indication of binding at asymmetric sites on helices. There may be more than one mode of binding. The discontinuity at $R = 0.07$ in the induced ellipticity maximum versus R plot for poly(U · U) (fig. 11) near the point of maximal helix formation may indicate a change in the nature of the binding that is dependent on the extent of saturation of this helix by the cations.

A strong argument has been made for a delocalized model of mono- and divalent cation binding to helices (counterion condensation) [25]. The immediate environment of a bound cation is essentially the same as that existing free in solution. The bound cation is completely hydrated and possesses free translational and rotational mobility. This model was also considered for cations of higher charge and more complex structure, such as polyamines and basic oligopeptides, where a conformational change could be induced in the cation upon binding to the nucleic acid. Such a change in ruthenium red could bring about the observed induced CD effects. This is, however, unlikely since the dye has a rigid, oxygen-bridged linear structure [12,13]. It is conceivable that the induced effects reflect a preferred average orientation of ruthenium red within an asymmetric electrostatic groove formed by the helical array of phosphates. We note also that each cation could bind adjacent DNA segments, as has been suggested for $Co(NH_3)_6^{3+}$-induced DNA condensation [17]. This likely occurs near the dye-phosphate charge neutralization point, where some precipitation was observed.

Within their asymmetric environment, the ruthenium red cations are mobile. The invariance of the induced CD effect across the lower transition of a biphasic melting profile (seen at sub-saturating levels of dye) indicates that there is a migration of cations from newly denatured to remaining helical regions, with no net change in binding. Upon melting through the upper transition, with the total denaturation of the nucleic acid, the effect is destroyed, since the cations are no longer bound to helical sites. The melting temperatures and magnitudes of the hyperchromic changes of the biphasic profiles can be used to estimate binding site size and association constant for the interaction of the dye with double helices.

4.2. Estimation of binding parameters

The data in fig. 2 clearly indicate that the portion of polyd(A-T) helix melting in the upper transition is a linear function of [dye], suggesting that the hyperchromic change of that transition reflects the availability of cations for binding to helical regions. If the affinity of the cations for the helices is sufficiently high, then up to the point of saturation, effectively all of the dye molecules are bound prior to denaturation. The fraction of helix melting at the higher transition ($\equiv f$) is proportional to R, allowing us to calculate the average number of helical residues apparently occluded by each dye molecule, n_h,

$$n_h = f/R, \qquad (1)$$

where

$$f = \Delta A_{260}^{(2)}/\Delta A_{260}^{(\mathrm{total})}. \qquad (2)$$

$\Delta A_{260}^{(2)}$ and $\Delta A_{260}^{(\mathrm{total})}$ are the hyperchromic changes of the higher and total transition, respectively. n_h was calculated from the data displayed in fig. 2 (where 52°C was taken as the dividing point between lower and higher transitions). With the exception of the data at the two lowest R values, where there may be greater error in determining f, n_h was found to be 7.2 ± 0.5 residues, or 3.6 base pairs.

Another parameter which is easily obtained from the ruthenium red--polyd(A-T) melting data, and is illustrative of the very high affinity of the dye for double helices, is R_{eff}, the effective ratio of ruthenium red to nucleotide of remaining helix upon completion of the lower transition (52°C). If we make the assumption that, at subsaturating levels, all dye molecules are bound to the helix, then we may define R_{eff} as

$$R_{\mathrm{eff}} = R/f. \qquad (3)$$

Comparison with eq. (1) shows that R_{eff} is equivalent to $1/n_h$, and the data of fig. 2 yield (at $R > 0.022$) $R_{\mathrm{eff}} = 0.14 \pm 0.01$. The very small variation in R_{eff} and n_h suggests that the remaining double-stranded regions are saturated at 52°C, and the affinity of the cations for the helix is sufficiently high so that essentially all the dye molecules in solution are bound at this point.

A similar calculation cannot be performed for the ruthenium red–poly(U) melting data, since, as we have shown, maximum hyperchromicity in the "higher" transition is reached at an R significantly below the point of saturation indicated by the T_m-enhancement and visible CD data (figs. 8–11). However, the linear rise in hyperchromicity at $0 < R < 0.07$ seen in fig. 8 indicates a high affinity of the dye molecules for the poly(U · U) helix.

An estimate of the association constant of ruthenium red for polyd(A-T) in the low salt buffer employed in these studies can be obtained using the relationship of McGhee ([7], eq. (6) of that paper; see also Crothers [26]),

$$\frac{1}{T_m^0} - \frac{1}{T_m} = \frac{\mathcal{R}}{\Delta H} \ln\left\{\frac{(1 + K_h L)^{1/n_h}}{(1 + K_c L)^{2/n_c}}\right\} \tag{4}$$

where T_m^0 is the melting temperature of the helix in the absence of added dye, T_m is the melting value at a given R value high enough to produce monophasic melting, $\mathcal{R}$ is the gas constant, ΔH is the enthalpy change upon helix denaturation, taken to be 8 kcal/base pair, K_h and K_c are the association constants of the dye for helix and coil binding sites, L is the free ligand (dye) concentration upon helix melting, and n_h and n_c are the occluded binding site sizes of helix and coil in base pairs and bases, respectively. If we ignore any significant dye–coil binding (which, based on the polyd(T) competition experiments, is certainly very minor compared to the dye–helix interaction), eq. (4) rearranges to

$$K_h = \exp\left\{\left(\frac{1}{T_m^0} - \frac{1}{T_m}\right)\frac{\Delta H}{\mathcal{R}} n_h\right\}^{-1} \Big/ L \tag{5}$$

Using the T_m data at $R = 0.134$ with $n_h = 3.6$ base pairs we calculate $K_h \sim 1 \times 10^7$ M^{-1}. Eq. (5) does not take into account the effect of overlapping binding sites at $n_h > 1$, which leads to an overestimation of K_h [7]. However, for large K_h ($K_h L > 100$), there is a relatively small discrepancy [7]. The calculated value of K_h is more likely a lower limit since the T_m observed in the presence of saturating levels of dye would likely be somewhat higher were ruthenium red heat-insensitive.

In eq. (5), any uncertainty in n_h is increased exponentially as uncertainty in K_h. Although we saw no direct evidence for more than one mode of binding to polyd(A-T), it is conceivable that the cations might initially occlude more than 3.6 base pairs (giving a larger value of K_h), but upon partial helix denaturation, the site size is reduced to this figure. Certainly, it is clear that the dye molecules can fully stabilize the poly(U · U) helix at less than saturating levels. The mode of binding and occluded site size under these conditions may be different from that occurring at $R \geqslant 0.07$, where the helix is fully formed. This is explicitly seen in the poly(U) system as a change in $[\Theta]_{557}$ calculated with respect to [ruthenium red] (fig. 11, inset). The inconstancy of $[\Theta]_{562}$ calculated with respect to [dye], in the presence of polyd(A-T), may also be indicative of more than one binding mode for this system as well (fig. 5, inset).

The near-linear dependence of the induced CD effects for both polyd(A-T) and poly(U) (figs. 5 and 11) also suggests that the association constants are sufficiently high so that virtually all added ruthenium red up to the point of saturation is bound to helix. The extended Scatchard approach of McGhee and von Hippel [27], which yields association constants and site sizes cannot be applied to this CD data since the concentration of free dye, which is required for the calculation, is ~0 up to the saturation point.

The small deviation from linearity seen with polyd(A-T) ($[\Theta]_{562}$ with respect to $[\text{polyd(A-T)}]_p$ versus R, fig. 5) at low R probably does not reflect lower than expected dye binding, since the variation of hyperchromicity of lower and upper transitions with increasing R is linear (fig. 2), and a lower than expected affinity would produce curvature of sign opposite to that observed. This deviation thus likely represents a non-linearity in the physical effect rather than in the extent of binding. The variation of $[\Theta]_{562}$ with respect to [dye] (fig. 5, inset) can be used to calculate correction factors for $0 < R < 0.17$, so that when multiplied by $[\Theta]_{562}$ with respect to $[\text{polyd(A-T)}]_p$, a linear $[\Theta]$ versus R plot results (not shown).

4.3. [Na$^+$] Dependence of ruthenium red–nucleic acid interaction

In order to determine the number of ion pairs involved in the dye–nucleic acid interaction, the [Na$^+$] dependence of the induced CD of the ruthenium red–polyd(A-T) mixture at $R = 0.112$ (fig. 6) was analyzed by the method of Record et al. [3]. Since the molar ellipticity with respect to dye concentration is variable with R, the reduction in ellipticity (calculated with respect to $[\text{nucleic acid}]_p$) upon increase in [Na$^+$] cannot be used as a direct indicator of the degree of dye binding. However, if it is assumed that the molar ellipticity with respect to ruthenium red is solely a function of [bound dye] : $[\text{polynucleotide}]_p$, and is not affected by changes in [Na$^+$], we can apply the correction factors calculated from fig. 5 (inset) to the calculation of the $[\text{ruthenium red}]_{\text{bound}}$: $[\text{nucleic acid}]_p$ at points on the [Na$^+$] dependence curve. We assume that at low

$[Na^+]$ all ruthenium red is bound to the nucleic acid, since $[\Theta]_{562}$ is invariant between ~0 and 0.10 M Na^+. Furthermore, no dye is bound at $[Na^+] > 0.22$ M, since $[\Theta]_{562} = 0$ beyond this point. The intermediate $[\Theta]_{562}$ values (with respect to $[\mathrm{polyd(A\text{-}T)}]_p$), when adjusted for variations in $[\Theta]$ calculated with respect to [dye], yield $[\text{ruthenium red}]_{\text{bound}}$. Knowing $[\text{ruthenium red}]_{\text{total}}$, $[\text{ruthenium red}]_{\text{free}}$ can then be calculated. Assuming no binding cooperativity, and a site size of 7.2 nucleotides, the association constant, K_h, can be calculated using eq. (10) of McGhee and von Hippel [27]. As Record, et al., have shown [3]

$$\frac{-\partial \log K_h}{\partial \log[M^+]} = k + m'\psi \qquad (6)$$

where k is the number of counterions released from the ligand upon binding, m' is the number of ion-pairs resulting, and ψ is a binding parameter equal to 0.88 for native DNA (and presumably the same or very similar for polyd(A-T)). With the uncertainty in n_h of ±0.5 nucleotides, we find a linear dependence (99% correlation coefficient) of $\log K_h$ on $\log[Na^+]$, with a slope of 9.4 ± 0.6 (data not shown). (In 0.165 M NaCl, about the mid-point of the sigmoidal portion of the polyd(A-T) data in fig. 6, $K_h = 2.5 \times 10^4\ M^{-1}$). If the correction factors are not used in the calculation, the slope is somewhat higher (10.6), but there is more deviation from linearity in the plot (96% correlation coefficient).

The stepwise association constant of small anions to ruthenium red are not known and thus no experimentally derived value of k can be used to determine m'. k must be at least 3 if we make the reasonable assumption that $m' \leqslant n_h$. The association constants of trivalent metal complexes with simple monovalent anions to form (1 : 1) ion pairs are in the order of 10 at an ionic strength of ~0.1 [28]. The ruthenium red cation, which formally consists of three positive Ru centers, would thus be expected to exhibit even higher association constants under the low (~0.01) ionic strength conditions employed in this study. Thus, it is likely that at least some counterion binding (and release) occurs. Alternatively, the method of Record et al. may not be strictly applicable to a cation with several positive centers, and a complicated ion pairing arrangement.

4.4. Ruthenium red as a probe of nucleic acid helical structure

The induced circular dichroism effect resulting when ruthenium red is interacted with nucleic acid helices might find useful application in the quantitation of exposed helical structure in complex particles such as nucleosomes or ribosomes. In a preliminary experiment with ruthenium red and erythrocyte monosomes ($R = 0.067$), an induced visible CD peak at 565 nm was observed to have ~1/4 the magnitude expected from naked, double-stranded DNA (Karpel, Shirley and McGhee, unpublished observations). When proteinase K was added to the cuvette (in the presence of dye), the size of the induced peak more than doubled in two hours. This suggests that as histones are degraded, more nucleic acid is exposed, and in turn, more dye is bound. Likewise, monosomes which had been predigested with proteinase K for 2 hrs showed an induced CD peak that was 3 -4 times higher than that seen with undigested material. Although the high charge of the ruthenium red cation could conceivably dislodge tightly bound proteins from the nucleic acid, the strong inhibition of the induced effect by histones suggests that this is minimal. Thus, in addition to its utility as a microscopic stain [10,11], ruthenium red might prove useful as a probe for the molecular aspects of protein-nucleic acid interactions.

Acknowledgement

The authors thank James McGhee and Jacques Fresco for useful discussions concerning this work, and Jon Widom and Robert Baldwin for sending us their manuscript prior to publication. This work was supported by research grant CA 21374 from the National Cancer Institute, National Institutes of Health, U.S. Public Health Service, and grants from the American Cancer Society, Maryland Division, and American Heart Association, Maryland Affiliate (all to R.L.K.). R.L.K. was a UMBC summer faculty fellow (1977).

The authors would also like to thank Matthey-Bishop, Inc. for the gift of a sample of ruthenium red used in preliminary experiments.

References

[1] J.R. Fresco, A. Adams, R. Ascione, D. Henley and T. Lindahl, Cold Spring Harbor Symp. Quant. Biol. 31 (1966) 527.
[2] G. Felsenfeld and H.T. Miles, Ann. Rev. Biochem. 36 (1967) 407.
[3] M.T. Record, Jr., T.M. Lohman and P. de Haseth, J. Mol. Biol. 107 (1976) 145.
[4] P.L. de Haseth, T.M. Lohman and M.T. Record, Jr., Biochemistry 16 (1977) 4783.
[5] R.L. Karpel and A.C. Burchard, Biochemistry 19 (1980) 4674.
[6] W.F. Dove and N. Davidson, J. Mol. Biol. 5 (1962) 467.
[7] J.D. McGhee, Biopolymers 15 (1976) 1345.
[8] R.L. Karpel, A.H. Bertelsen and J.R. Fresco, Biochemistry 19 (1980) 504.
[9] J.M. Fletcher, B.F. Greenfield, C.J. Hardy, D. Scargill and J.L. Woodhead, J. Chem. Soc. 1961 (1961) 2000.
[10] J.H. Luft, Anat. Rec. 171 (1971) 347.
[11] J.H. Luft, Anat. Rec. 171 (1971) 369.
[12] F.A. Cotton and G. Wilkinson, Advanced inorganic chemistry (3rd Ed., Interscience, New York, 1972) p. 1011.
[13] P.M. Smith, T. Fealey, J.E. Earley and J.V. Silverton, Inorg. Chem. 10 (1971) 1943.
[14] A.L. Stone, in: Methods in carbohydrate chemistry, Vol. 7, eds. R.L. Whistler and J.N. BeMiller (Academic Press, New York, 1976) p. 120.
[15] R.B. Inman and R.L. Baldwin, J. Mol. Biol. 5 (1962) 172.
[16] R.D. Blake, J. Massoulié and J.R. Fresco, J. Mol. Biol. 30 (1967) 291.
[17] J. Widom and R.L. Baldwin, J. Mol. Biol. 144 (1980) 431
[18] P.O.P. Ts'o, S.A. Rapaport and F.J. Bollum, Biochemistry 5 (1966) 4153.
[19] D.E. Jensen, R.C. Kelly and P.H. von Hippel, J. Biol. Chem. 251 (1976) 7215.
[20] E.G. Richards, C.P. Flessel and J.R. Fresco, Biopolymers 1 (1963) 431.
[21] W. Szer, J. Mol. Biol. 16 (1966) 585.
[22] J.C. Thrierr, M. Dourlent and M. Leng, J. Mol. Biol. 58 (1971) 815.
[23] S.B. Zimmerman, J. Mol. Biol. 101 (1976) 563.
[24] A.M. Michelson and C. Monny, Proc. Natl. Acad. Sci. USA 56 (1966) 1528.
[25] G.S. Manning, Quart. Rev. Biophys. 11 (1978) 179.
[26] D.M. Crothers, Biopolymers 10 (1971) 2147.
[27] J.D. McGhee and P.H. von Hippel, J. Mol. Biol. 86 (1974) 469.
[28] R.L. Karpel, N.S. Miller, A.M. Lesk and J.R. Fresco, J. Mol. Biol. 97 (1975) 519.